# A STUDY OF DYNAMIC NEAR-CRACK-TIP FRACTURE PARAMETERS BY DIGITAL IMAGE ANALYSIS

W. Peters, W. Ranson, J. Kalthoff, S. Winkler

## To cite this version:

W. Peters, W. Ranson, J. Kalthoff, S. Winkler. A STUDY OF DYNAMIC NEAR-CRACK-TIP FRACTURE PARAMETERS BY DIGITAL IMAGE ANALYSIS. Journal de Physique Colloques, 1985, 46 (C5), pp.C5-631-C5-638. 10.1051/jphyscol:1985581 . jpa-00224815

**HAL Id: jpa-00224815**

**https://hal.science/jpa-00224815**

Submitted on 4 Feb 2008

JOURNAL DE PHYSIQUE
Colloque C5, supplément au n°8, Tome 46, août 1985

# A STUDY OF DYNAMIC NEAR-CRACK-TIP FRACTURE PARAMETERS BY DIGITAL IMAGE ANALYSIS

W.H. Peters, W.F. Ranson, J.F. Kalthoff* and S.R. Winkler*

*College of Engineering, University of South Carolina, Columbia, SC 29208, U.S.A.*
**Fraunhofer Institut fur Werkstoff-Mechanik, Freiburg, F.R.G.*

Résumé - On discute la faisabilité à déterminer les paramètres de fracture de matériaux soumis à un impact, en utilisant des techniques photographiques à grande vitesse couplées avec un système de digitalisation des images par ordinateur. On présente le procédé d'obtention des données et la méthode d'analyse qui sont appliqués pour déterminer expérimentalement le champ des déplacements à la pointe de la fissure.

Abstract - The feasibility of quantifying fracture parameters for cracked body problems under impact loading through the use of high speed photographic techniques coupled with computer based digital image processing methods is discussed. The procedure for gathering data and the method of analysis which is applied to the experimentally determined displacement field in the crack tip region is presented.

## I - INTRODUCTION

The area of digital image analysis is receiving considerable attention in the general field of mechanics. In particular, several studies are being undertaken to investigate the near-crack-tip displacement and stress fields through the digital recording and subsequent processing of either random white light speckle phenomena or the photoelastic effect. In these studies, the displacement field data and the photoelastic data are analyzed using linear elastic theory to make estimations of the Stress Intensity Factor, $K_I$.

In this paper, the results of cooperative two year effort to develop a new experimental methodology to study the dynamic fracture mechanics problem is discussed. A Cranz-Schardin camera was used to record images on film of the crack tip region before and during the dynamic impact of a standard three-point bend fracture specimen made from Araldite B. A random pattern of black and white spots had been applied to the surface of the specimen in the crack tip region. The images were then digitized using a system which consist of a video camera, digitizing computer, and a mainframe computer with associated peripheral components. A typical digitized white light speckle pattern duplicates the random character of the black and white pattern. The digitized intensity levels are recorded at each spatial pixel (picture element) location of the video camera which was used to record the images and for the present system are specified by a 512 x 512 array of numbers.

The dynamic data which is in digital form can be analyzed with established digital correlation procedures to yield the local crack tip displacement field. The correlation procedure (which is explained later) is normally used to estimate the component of the displacement vector which is perpendicular to the crack plane. This displacement is then known at discrete pixel locations in a local region which includes the crack tip position.

A procedure has been developed to estimate the Stress Intensity Factor. This procedure is based on a least square error analysis method and uses a comparison of the raw displacement data and the theoretical solution for the static cracked body problem to estimate $K_I$ for the dynamically impacted three point bend specimen. Higher order effects are included in the theoretical solution to account for the finite size of the experimental field data which is used for the $K_I$ estimate. Results obtained for the impact of a three point bend fracture specimen are compared with the experimental results from the shadow-optical method of caustics.

## II - BACKGROUND FOR IMAGE CORRELATION AND STRESS INTENSITY FACTOR DETERMINTION

The procedure which is used to correlate the successive images obtained during a dynamic event has been presented else where /1/, and for clarity, will be repeated here. Also the numerical procedure for obtaining the Stress Intensity Factor from the displacement data in the crack tip region is summarized in the following discussion.

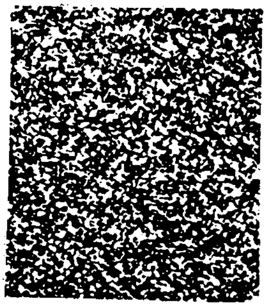

Figure 1. White Light Speckle

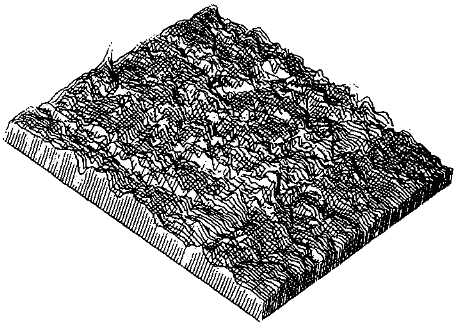

Figure 2. Digitized White Light Speckle

A digital image of a body is simply a discrete intensity record of the light levels present at various positions on a body (for more detail see /2/ and /3/). The sampling interval size is controlled by the detector size and image magnification. A typical object with a random white light speckle pattern is shown in Figure 1. The digital intensity record for a pattern similar to the one shown in Figure 1 is presented in Figure 2. If one supposes that the intensity pattern after deformation is related through the object deformation of the intensity pattern recorded before deformation, then this suggests a correlation of two images to detect the image differences (e.g., the object deformation). Thus, consider the intensity "surfaces" f(x,y) and f*(x*,y*), as shown in Figure 3. The subset shown is mapped to a new position x*, where x* is related to x by the local deformation. If one considers a small subset so that the affine mapping

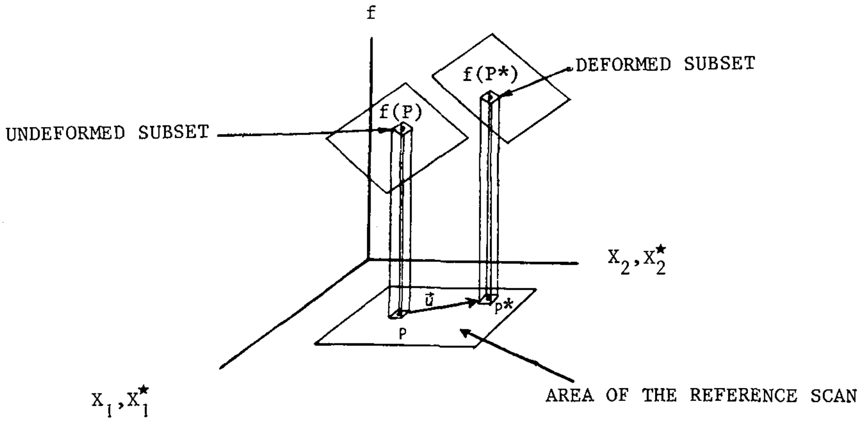

Figure 3. Intensity Surface of Images

$$x^*_i = x_i + U_i + \frac{\partial U_i}{\partial x_j} \nabla x_j \quad \text{-------} \quad i,\ j=1,\ 2 \qquad (1a)$$

is valid, then the deformed subset can be written

$$f^*(x^*,y^*) = f^*\ (x_1 + \frac{\partial U_1}{\partial x_1} dx_1 + \frac{\partial U_1}{\partial x_2} dx_2,\ \ldots) \qquad (1b)$$

Though there are several methods for correlation of one image to another, the one chosen for this work is the "least-squares" correlation and is written

$$C\ (U_i, \frac{\partial U_i}{\partial x_j}) = \sum_{\Delta M} [f^*(x^*_1, x^*_2) - f(x_1, x_2)]^2 \qquad (2)$$

where $\nabla M$ is the subset of interest from the digital image. The values of $U_i$ and $\partial U_i / \partial x_j$ which minimize (2) are the values of local deformation incurred by the object.

The correlation procedure can then be applied over the local region of interest. For the fracture mechanics problem, in-plane displacement data is obtained for a region which contains the crack tip location. As explained in the next section, this displacement data can be used to make an estimate of the mode I ($K_I$) stress intensity factor (SIF).

## III - ESTIMATION PROCEDURE FOR STRESS INTENSITY FACTOR

The Westergaard solution /4/ and /5/ for the cracked body problem can be used to specify the displacment field in the region of the crack tip. The experimental procedure discussed in this paper can be employed to measure the displacement field in this same near-crack tip region. This section will discuss a least squares error analysis procedure which uses full field local crack tip displacement data for estimating the Stress Intensity Factor.

Assume that a parameter of interest (F) can be represented in an analytical fashion as

$$F(x_1,x_2) = \sum_{i=1}^{n} A_i f_i(x_1,x_2) \qquad (3)$$

where $x_1,x_2$ represent planar coordinate locations, $f_i$ is a known function of coordinate position and the unknown A coefficients are taken to be independent of the $f_i$'s. Now let $u_j$ be the data measured at each point which corresponds to the parameter of interest. Then, the error between the parameter of interest and the measured data at each particular point in the $x_1,x_2$ can be defined as

$$E_j = [\sum_{i=1}^{n} (A_i f_i(x_{1j},x_{2j})) - u_j(x_{1j},x_{2j})]^2 \qquad (4)$$

The total error for the whole field of data becomes

$$E_T = \sum_{j=1}^{m} E_j = \sum_{j=1}^{m} [\sum_{i=1}^{n} (A_i f_i(x_{1j},x_{2j})) - u_j(x_{1j},x_{2j})]^2 \qquad (5)$$

Since the $f_i$'s have been taken to be known functions of position, then the total error is related only to the coefficients, $A_i$. In order to minimize the error, the partial derivatives of the total error with respect to the coefficients are taken and set equal to zero as follows,

$$\frac{\partial E_T}{\partial A_i} = 0 = \sum_{j=1}^{m} [2 \{ \sum_{i=1}^{n} (A_i f_i(x_{1j},x_{2j})) - u_j(x_{1j},x_{2j})\} f_i(x_{1j},x_{2j})] \qquad (6)$$

The set of equations generated in this fashion contain unknowns (the $A_i$'s). Solution of the n equations for the unknown $A_i$'s forces the best possible analytical representation of the measured data.

For the mode I fracture problem discussed in this paper (with $x_1$, in the direction of crack advance and $x_2$ perpendicular to the crack plane), the function F is represented by the series solution for the $U_2$ displacement field ($K_I$-controlled) in the neighborhood of the crack tip, plus terms which analytically represent contribution to the displacement field because of the physics of the test set-up (i.e., in-plane rigid body translation and rotation). As an illustration of the estimation procedure, consider the following. Let F be a function of the $r,\theta$ polar coordinates at the crack tip ( measured from $x_1$ axis and positive counterclockwise) and be given by

$$F(r,\theta) = A_1 f_1(r,\theta) + A_2 f_2(r,\theta) \qquad (7)$$

where

$$f_1(r,\theta) = \frac{r^{\frac{1}{2}}}{G\sqrt{2\pi}} \sin\frac{\theta}{2} \left(\frac{2}{1+\nu} - \cos^2\frac{\theta}{2}\right)$$

$$f_2(r,\theta) = 1$$

For this example, only the leading term ($A_1 f_1$) of the series representation of the displacement field in the crack-tip region has been included. Therefore, $A_1$ becomes equal to $K_I$, the mode I Stress Intensity Factor. The second term represents a rigid body motion. For this example, the minimization yields the equations

$$A_1\left[\sum_{j=1}^{m} f_1^2(r_j,\theta_j)\right] + A_2\left[\sum_{j=1}^{m} f_1(r_j,\theta_j)\right] = \left[\sum_{j=1} u_j f_1(r_j,\theta_j)\right] \qquad (8)$$

$$A_1\left[\sum_{j=1}^{m} f_1(r_j,\theta_j)\right] + A_2\left[\sum_{j=1}^{m} (1)\right] = \left[\sum_{j=1}^{m} u_j\right]$$

which can be solved for $A_1$ ($K_I$) and $A_2$ (rigid body motion).

The value of Stress Intensity Factor which is obtained by this analysis procedure is based upon a static analysis method. However, the inclusion of higher order terms related to the dynamic effects could easily be accomplished when the form of these terms has been established in future research.

## IV - EXPERIMENTAL PROCEDURE AND RESULTS

The experiments to obtain the data for this study were performed in the laboratory of the German authors and were very similar to the experiments which have been previously performed /6/, /7/ to obtain the dynamic stress intensity factor for the impacted three-point bend specimen. The specimen which was used in the experiments is shown in Figure 4. This specimen was machined from Araldite B and had the

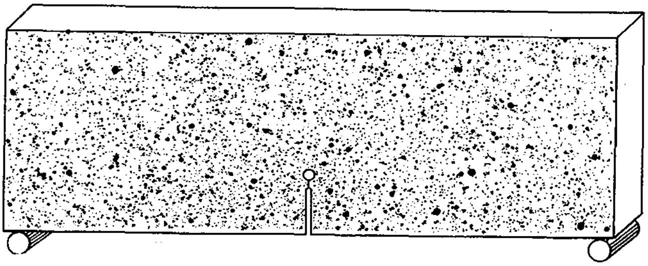

Figure 4. Three Point Bend Specimen

overall dimensions of 400 x 100 x 10 mm. The specimen contained a 30mm "crack" which terminated in a 0.7 mm root radius hole. A finite root radius hole allowed the specimen to store energy and prevented the crack from running. The specimen was then sprayed with a fine mist of black spray paint which created a random pattern of various size black pots in the crack tip region.

Before impact of the specimen, no load images of the crack tip region were recorded on Eastman Kodak Graphic Art Film through the use of a Cranz-Schardin high speed camera system. The Cranz-Schardin system consists of a 24-spark unit which has a framing rate of 0.2 frames per second (fps) to 1 x 10 fps. The duration of each spark is less than 1$_{\mu}$s. The light from the sparks is collected onto a 24-lens array imaging system by a concave mirror.

A schematic of the test configuration is shown in Figure 5. The 24-lens array system is focused on the surface of the specimen which contains the random pattern on sprayed dots. The light from the sparks traverse a path through the specimen.

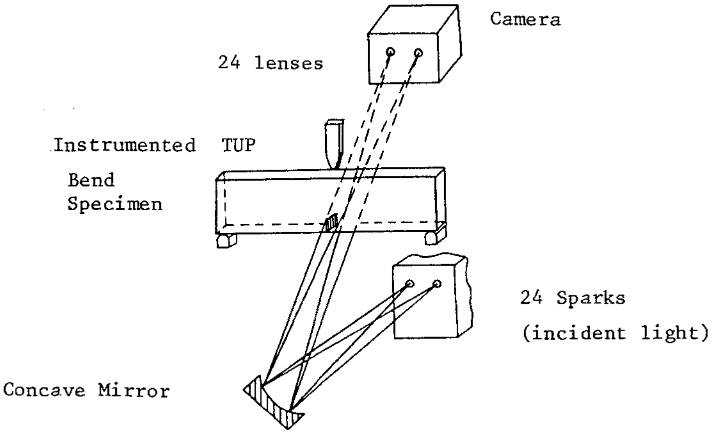

Figure 5. Optical Arrangements for High Speed Registration of Impact Bend Spectrum

The specimen was then impacted by a 1.25 kg mass with an impact velocity of 1m/s. The Cranz-Schardin system was again used to record images during the impact event. A set of double images was required to eliminate the introduction of false displacements into the data because of geometry differences in the optical configuration which was utilized in the experiments.

The no load and impacted images of the crack tip region were then digitized using DAGE MTI Video Camera and a VICOM digitizer at the University of South Carolina. This digitizing computer (VICOM) digitizes with a gray level resolution of 256 and a spatial resolution of 512 x 512 pixels (picture elements). Magnification of the video camera determines the size of the displacement which is measurable. The magnification in these experiments was approximately 50 pixels per mm of true specimen length. The displacements which measured in the crack were on the order of 0.01mm.

The image correlation procedure which was discussed in the previous section was used to determine the displacement field in an area near the crack tip. This area was approximately 8 mm square and contained the crack tip and the region near the opening crack surfaces. The component of displacement perpendicular to the crack plane $U_2$ (in $x_1$ direction) was determined by the correlation procedure. This displacement was then used in the error analysis procedure (discussed in previous section) to predict dynamic stress intensity values ($K_I^{dyn}$) at various times during the impact event.

The predicted $K_I^{dyn}$ values for this study are shown in Figure 6. The estimation procedure included higher order terms in the analysis and the predicted $K_I^{dyn}$ values were chosen when convergence (as the number of higher order terms increased) to a constant value of $K_I^{dyn}$ was observed.

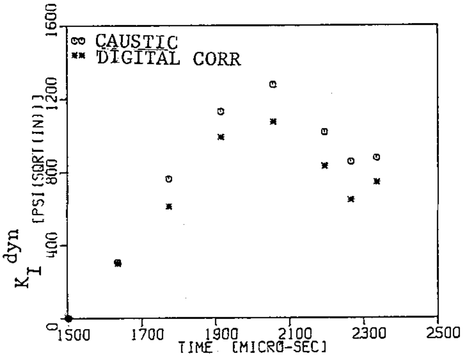

Figure 6. Comparison of $K_I^{dyn}$ for Caustic and Digital Correlation technique

In Figure 6, the $K_I^{dyn}$ values from the digital correlation method are compared with the results from the experimental method of caustics /7/. The comparison shows that identical trends are noted in the data. However, the results predicted in the current work are 2%-20% below the caustic results. The reason for this difference can probably be attributed to the experimental setup which was used in the current experiments. The light traverses the thickness of the specimen as shown in Figure 5. Because of the high stress field and geometrical changes in the specimen surface. This causes a deflection of the light (much like that which occurs in the caustic setup--but much smaller here) which is collected to form the impacted image in the present study. This deflection would cause a false displacement which cannot be acounted for with the present analysis. Experiments are currently underway to photograph only the surface of the specimen and thus eliminate this effect which at the present time cannot be quantified.

## V - CONCLUSIONS

The digital image processing method introduced in this paper has been shown to hold some promise for studying dynamic fracture problems. Further development of the experimental method coupled with the current analysis procedure should provide a new experimental method to obtain the displacement field and fracture parameters for elastic and elastic-plastic dynamic fracture problems.

## ACKNOWLEDGEMENTS

The authors would like to thank Professor M. Sutton, Mr. Steve McNeill and Mr. Javid Novinbakht at the University of South Carolina and Mr. W. Bohme at the Fraunhofer Institut Fur Werkstoffmechanik for their valuable contributions to this work. The authors would like to acknowledge the encouragement of Dr. Warren Thompson and the support of the National Science Foundation under grant #INT-8214093, and also the encouragement of Dr. Clifford Astill and the support of the National Science Foundation under grant #MEA 82-14040.

## REFERENCES

/1/ McNeill, S.R., Peters, W.H., Sutton, M.A. and Ranson, W.F., Proc. of SECTAM XII (1984) 188.

/2/ Peters, W.H., and Ranson, W.F., Proc. W.F., Optical Engineering 21 (1982) 427.

/3/ Sutton, M.A., Wolters, W.J., Peters, W.H., Ranson, W.F. and McNeill, S.R., Image and Vision Computing 1 (1983) 133.

/4/ Westergaard, H.M., J. of Appl. Mech. 61 (1939) A49.

/5/ Paris, P.C., and Sih, G.C., ASTMSTP381 (1965) 30.

/6/ Bohme, W., Kalthoff, J.F., and Winkler, S., Sitzung des Arbeitskreises Bruchvorgange in DVM (1980) 233.

/7/ Bohme, W., and Kalthoff, J.F., Int J. of Frac. 20 (1982) R139.